A Label-Free Approach to Identify Inhibitors of α4β7-Mediated Cell Adhesion to MadCAM

MICHAEL P. BOVA,[1]* LAN NGUYEN,[1]* WILLIAM WALLACE,[1] CAROLINE GARRIDO,[1] YING-ZI XU,[1] CHRIS SEMKO,[1] KELLY COCKCROFT,[2] ERIC SANDBERG,[2] and FREDERIQUE BARD[1]

Traditionally, cell adhesion assays are performed in a manual workstation format using fluorescence-based readouts. Herein, the authors describe a label-free homogeneous assay to identify inhibitors of α4β7 integrin-mediated cell adhesion to its ligand, the mucosal addressin cell adhesion molecule (MadCAM), using the SRU BIND platform. The biosensor is optically based and comprises a subwavelength polymer grating. The assay was validated using standard compounds and an α4 blocking antibody and correlated very closely with the manual assay format when running a battery of test compounds of varying potencies. Cell adhesion was strictly dependent on the presence of divalent cations where Mg^{2+} was greater than Ca^{2+} at promoting cell adhesion. This homogeneous and label-free format exhibited low variability with a calculated Z′ of 0.6. In addition to measuring α4β7-mediated 8866 cell adhesion to MadCAM, the authors also demonstrate that this platform can measure adhesion of Jurkat cells expressing α4β1 to the vascular cell adhesion molecule. Thus, the SRU BIND platform is widely applicable to measuring cell adhesion events mediated by other integrins binding to their receptors in an assay format that is amenable to high-throughput screening. (*Journal of Biomolecular Screening* 2011;16:536-544)

Key words: label free, cell adhesion, MadCAM, cell-based assay, inflammatory diseases

INTRODUCTION

Integrins are cell adhesion molecules that play an important role in a number of biological processes, including hemostasis and wound healing, cell migration and trafficking, cell differentiation, and immune responses.[1,2] Integrins exist as heterodimers containing two noncovalently bound type I transmembrane alpha and beta subunits that both consist of an extracellular domain, a single-spanning transmembrane domain, and a short intracellular domain.[3]

Integrins can and do exist in different conformations or activation states. Based on studies using crystallography, nuclear magnetic resonance (NMR), and electron microscopy, integrins can adopt a bent conformation (low affinity for substrate), an extended conformation with closed headpiece (intermediate affinity), and an extended conformation with open headpiece (high affinity).[4] These conformations are in equilibrium with each other, yet the equilibrium can be shifted by cytoplasmic signals by what is known as inside-out signaling.[5,6] Platelet aggregation represents a well-studied example of inside-out signaling where, in the resting state of the platelet, α2β3 integrin is in a low-affinity conformation for its ligand, soluble fibrinogen.[7] Following platelet activation by agonists such as thrombin, adenosine diphosphate (ADP), or epinephrine, which signal through G-protein-coupled receptors (GPCRs), α2β3 integrin shifts to a high-affinity conformation for fibrinogen and platelet aggregation results.[8] A number of signal transduction pathways can converge to enhance integrin affinity for their ligands where it has been elegantly shown that talin binding to the integrin β tail is an essential final step in stimulating inside-out activation.[9] Inside-out-generated integrin conformational changes are also required for arrest of rolling leukocytes on vascular endothelium where endothelial-based chemokines binding to chemokine receptors (GPCRs) on lymphocytes rapidly enhance integrin adhesiveness.[10,11]

Integrins are bona fide signal-transducing receptors that convey information regarding local environment and adhesive state after engagement with their ligand in a process known as outside-in signaling.[12] Binding of the integrin to its ligand also stabilizes the

[1]Department of Biology, Elan Pharmaceuticals, South San Francisco, CA, USA.
[2]SRU Biosystems, Woburn, MA, USA.
*These authors contributed equally to the work.
Received Dec 7, 2010, and in revised form Jan 11, 2011. Accepted for publication Jan 11, 2011.

Supplementary material for this article is available on the *Journal of Biomolecular Screening* Web site at http://jbx.sagepub.com/supplemental.

Journal of Biomolecular Screening 16(5); 2011
DOI: 10.1177/1087057111399337

extended conformation. Integrin ligands are multivalent, which facilitates integrin clustering, which has been shown to be important for outside-in signaling.[13] Integrin signaling serves to initiate or modulate pathways involved in proliferation, survival/apoptosis, shape, motility, gene expression, and differentiation.[14,15]

Integrins are not always activated and in fact exist most of the time in an inactivated or off state. When integrins are not regulated or are constitutively in the activated state, pathological conditions can occur. For example, whereas platelet aggregation is an important part of wound healing, aberrant activation of platelets, mediated by activated αIIbβ3 integrin, is a primary cause of arterial thrombosis.[16] Integrins facilitate the movement of immune cells to their site of action in a process called extravasation,[17] which consists of a tightly regulated orchestration of adhesion and then de-adhesion of immune cells to substrates and blood vessel walls. It has been shown that mutations in α4β7 integrin can modulate the extent of lymphocyte trafficking into the gut, thus providing a mechanism to explain the wide variation of immune responses in patients suffering from inflammatory disorders such as ulcerative colitis and Crohn's disease.[18] Finally, αvβ3 integrin is constitutively expressed on several malignant tumor cells where a correlation exists between level of αvβ3 integrin expression and tumor invasiveness, particularly in liver metastases and melanomas.[19]

In terms of inflammatory diseases, antagonism of α4 integrin has been shown to be an effective therapy for multiple sclerosis (MS) and Crohn's disease,[20,21] for which natalizumab, a humanized antibody against the α4 integrin subunit, was approved for both indications. The impressive efficacy of natalizumab provides unequivocal validation of α4 integrin as a tractable pharmaceutical target.[22] Animal models and early clinical data would support α4 antagonism as a target in other inflammatory diseases such as asthma, inflammatory bowel disease, and rheumatoid arthritis.[23]

Despite the attractiveness of integrins as pharmaceutical targets, there is not a plethora of higher throughput and robust assays to measure their activity. Although plate-based fluorescence formats as well as fluorescence-activated cell sorting (FACS) have been successful for measuring cellular adhesion events, these assay formats either involve tedious manual manipulation that limits their throughput or use instrumentation that are not amenable to high-throughput screening (HTS). Herein, we describe a label-free, high-throughput, and robust assay to identify small-molecule inhibitors of α4β7-mediated cell adhesion to 8866 cells.

MATERIALS AND METHODS

Reagents

The antihuman Fc antibody used for MadCAM capture (cat. I-6260) was obtained from Sigma (St. Louis, MO). Recombinant MadCAM engineered to contain an Fc region can be purchased from R&D Systems (Minneapolis, MN). In-house-produced MadCAM-Fc was expressed in HEK293 cells and purified with a Protein A column followed by gel filtration on a Superdex-75 column. Corning Costar 96-well enzyme immunoassay (EIA)/radioimmunoassay (RIA) flat-bottom high-binding plates (cat. 3590; Corning, Corning, NY) were used for the manual cell adhesion assay. Titanium dioxide (TiO_2) 384-well plates were obtained from SRU Biosystems (Woburn, MA). 8866 and Jurkat cells were purchased from the American Type Culture Collection (ATCC, Rockville, MD). Glutamine, penicillin, and streptomycin were all purchased from Gibco-Invitrogen (Carlsbad, CA). Fetal bovine serum (F0926) was obtained from Sigma. Calcein AM dye was purchased from Invitrogen (Carlsbad, CA). All other regents were acquired from Sigma.

Cell culture

8866 and Jurkat cells were cultured in RPMI 1640 media from Gibco-Invitrogen supplemented with 10% fetal bovine serum (FBS), 2 mM L-glutamine, 50 IU/mL penicillin, and 50 μg/mL streptomycin. Cells were passaged twice/week at a 1:10 ratio of cell suspension to fresh media.

Description of BIND Reader

The SRU BIND Reader is a novel label-free plate-based reader that is ideally suited for cell-based assays. Similar to surface plasmon resonance biosensors, this technology also uses a change of index of refraction at the biosensor surface to measure molecular interactions. However, in contrast to other optically based biosensors, the SRU BIND technology uses photonic crystal biosensors composed of a subwavelength polymer grating coated with a high refractive index material (TiO_2).[24] The biosensor surface resonantly reflects a single wavelength that is modulated by the adsorption of biomaterial to the sensor surface. The SRU BIND Reader uses a collimated broad wavelength light source to illuminate the biosensor surface at the bottom of each well of a SBS-standard plate. Reflected light is collected and transmitted by an optical fiber to a spectrometer, which measures the wavelength of reflected light. In the case of cell adhesion assays, specific adherence of cells to the bottom of the coated biosensor causes a shift in the wavelength of reflected light, which is denoted as a shift in peak wavelength value (PWV). Cells that passively settle on the plate do not elicit PWV shifts to the same magnitude as cells that specifically adhere to matrix coated on the biosensor surface. Treatments to cells that strengthen or weaken adhesion will result in an increase or decrease in PWV shift, respectively. Passive settling is defined by the amount of PWV shift observed when cells settle on a bovine serum albumin (BSA)–blocked TiO_2 plate and is considered background.

SRU BIND adhesion assay format

The cell adhesion assay is a 2-day assay where on day 1, 8866 cells were split from the carrying flask using a 1:4 ratio

of 8866 cell suspension to fresh medium and cultured overnight. TiO_2-coated 384-well plates were hydrated in water and then washed with 20 mM HEPES (pH 7.4) containing 140 mM NaCl, 1 mM $CaCl_2$, and 1 mM $MgCl_2$ (buffer 1). Plates were prepared for experimentation by incubating an antihuman Fc antibody diluted 1:500 in buffer 1 in the TiO_2 plate for 1.5 h. Plates were then blocked with buffer 1 that was supplemented with 4% heat-inactivated BSA for 1 h and washed with buffer 1, and unless otherwise noted, recombinant MadCAM, engineered to contain an Fc region, was incubated on the plate at a concentration of 0.15 μg/mL overnight at 4h°C.

On day 2, compounds starting at a top concentration of 2 mM were diluted with DMSO 1:3 using the Biomek 2000 Laboratory Automation Workstation from Beckman (Brea, CA). Compounds were then diluted 50 × with 20 mM HEPES (pH 7.4) containing 140 mM NaCl, 1 mM $CaCl_2$, 1 mM $MgCl_2$, and 0.3% BSA (buffer 2) in a Costar #3363 V-bottom plate. 8866 cells were harvested, counted, and diluted with buffer 2 to a concentration of 8×10^6 cells/mL, and then equal volumes of 8866 cells, as well as compounds diluted in buffer 2, were incubated together for 30 min at room temperature. The SRU BIND plate was washed with buffer 1 and aspirated to remove any nonbound recombinant MadCAM, and then 25 μL of buffer 2 containing 1% DMSO was added to the MadCAM-coated TiO_2 plate, and a prescan baseline measurement was recorded on the SRU BIND Reader. To initiate cell adhesion, 25 μL of the cell/compound mixture (60K cells/well final) was added to the MadCAM-coated TiO_2 plate, which represented a 200 × final dilution of compound. Kinetic measurements of PWV shift were then recorded by the SRU BIND Reader every 30 s up to 90 min unless otherwise noted. IC_{50} values were calculated by defining 100% inhibition as the PWV shift observed when cells were pretreated with a saturating concentration (15 μg/mL) of the α4 blocking antibody (known as 21/6), where 0% inhibition (maximal cell adhesion) was defined as the PWV shift observed when cells were added alone to the MadCAM-coated well. All conditions contained a 1% DMSO final concentration in-well.

Manual cell adhesion assay format

On day 1, 8866 cells were prepared similarly as performed for the SRU BIND adhesion assay format. A Costar 96-well flat-bottom plate was prepared for experimentation by immobilizing an antihuman Fc antibody diluted 1:500 in buffer 1 for 1 h. Plates were then blocked with buffer 2 and washed, and recombinant MadCAM was incubated on the plate at a concentration of 0.15 μg/mL in phosphate-buffered saline (PBS) supplemented with 0.9 mM $CaCl_2$ and 0.5 mM $MgCl_2$ overnight at 4 °C.

On day 2, 8866 cells were labeled with calcein-AM (10 μg/mL) for 30 min at room temperature, and then cells were centrifuged at low speed to remove dye not captured in cells and then resuspended at 2×10^6 cells/mL in buffer 2. Compounds were prepared similarly as for the SRU BIND adhesion assay format where 100 μL of the cell/compound mixture was then added to the washed MadCAM-coated plate for 30 min at a final cell density of 100K cells/well. Plates were then carefully washed two times manually and then two additional times gently with a manifold. Cells remaining on the bottom of the plate were considered to have adhered to MadCAM, whereas cells that had been washed away were considered to be nonadherent. Adherence of cells to the MadCAM-coated plate was quantified by measuring the calcein fluorescence at the bottom of the plate using a Cytofluor 4000 plate reader from PerSeptive Biosystems (Framingham, MA) with excitation and emission wavelengths set at 485 and 530 nm, respectively, and gain at 47.

Description of BIND Scanner

The BIND Scanner enables high-resolution label-free imaging of cell attachment and adhesion signals. The BIND Scanner images a narrow segment of a photonic crystal optical biosensor at the bottom of a SBS-standard plate onto the slit of a custom imaging spectrometer. Changes in the strength and position of cell binding to the optical biosensor change the wavelength reflected back. At over a thousand individual points on the slit, the optical spectrum of the light reflected from the biosensor is measured, and the peak wavelength that is contained in the reflection is determined. From there, the point-to-point PWV is assembled into a line image, with lighter gray representing higher wavelength and darker gray representing lower wavelength. A mechanical translation stage scans the plate over the optics in a raster fashion, assembling successive line images into a full two-dimensional image of each well within a plate.

Imaging cell adhesion on the BIND Scanner

8866 cells incubated in the presence or absence of an α4 blocking antibody or compound 1 were then added to MadCAM-coated BIND plates at a density of 60 000 cells/well. After 45 min, wells were read on the BIND Scanner to image cells that had adhered to MadCAM. A 1-mm^2 area was read by the scanner at a 3.75-μm resolution.

BIND Scanner data processing

The BIND Scanner software performs a smoothing on the data to remove background artifacts from causing false positives. The smoothed image is then thresholded (min/max for PWV shift). Any pixels that fall outside the min/max range are ignored. Pixels that are within the min/max range are checked against cell size parameters. A cell is defined as a continuous region of pixels. The size parameters identify the minimum and maximum sizes of a continuous pixel region that are then identified as a cell. Any pixels within the min/max threshold range that do not fall within the size parameters are ignored, resulting in only valid

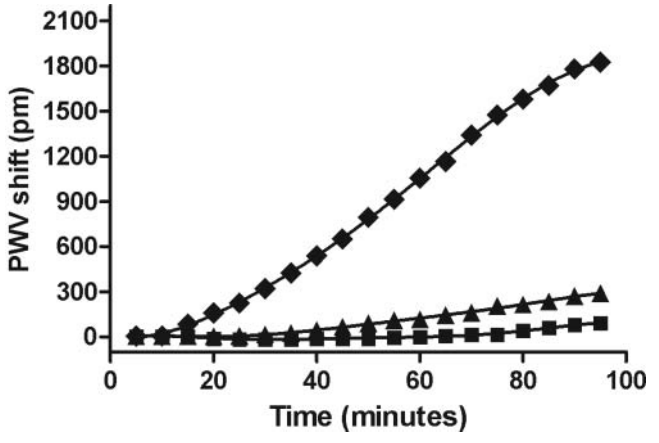

FIG. 1. Measuring the kinetics of 8866 cell adhesion to MadCAM using the SRU BIND platform. 8866 cells were added to each well of a SRU BIND plate under the following conditions: (▲) Fc capture antibody alone, (◆) Fc capture antibody + 0.15 μg/mL MadCAM, and (■) Fc capture antibody + 0.15 μg/mL MadCAM with 10 μg/mL α4 blocking antibody added to cells. Data were normalized to the peak wavelength value (PWV) shift observed on the bovine serum albumin–coated plate alone. This experiment has been repeated on more than three independent occasions with similar results.

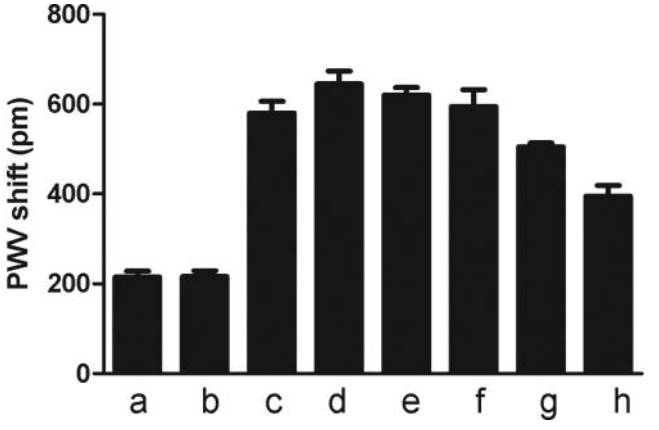

FIG. 2. Determining optimal Fc capture antibody dilution. In data generated for this figure, the MadCAM concentration was kept constant at 0.3 μg/mL, whereas the Fc capture antibody was incubated in the BIND plate at the dilutions indicated: (a) bovine serum albumin alone, (b) MadCAM alone, (c) Fc capture antibody dilution of 1:500 + MadCAM, (d) 1:1000 dilution, (e) 1:2000 dilution, (f) 1:4000 dilution, (g) 1:8000 dilution, and (h) 1:16 000 dilution. The peak wavelength value (PWV) shift indicated in the figure represents an endpoint measurement taken after 45 min of incubation of 8866 cells in the MadCAM-coated plate. All data represent the mean ± SD, $n = 4$.

cell pixels. Pixels meeting cell parameters are pseudocolored for image clarity. The software calculates the strength of cell adhesion by first determining the average pixel value (PWV shift) for all the pixels within a well that were defined as a cell. The software then determines the average of the cell values to determine adhesion strength of the cells in a given well.

RESULTS

Monitoring adhesion of 8866 cells expressing α4β7 to MadCAM using the SRU BIND platform

8866 cells are a human B cell line that endogenously expresses the α4β7 integrin. α4β7 integrin has been characterized as a ligand for MadCAM where interaction of α4β7 integrin with MadCAM is important for lymphocyte homing to the gut.[25] In **Figure 1**, we have examined the kinetics of 8866 cell adhesion to MadCAM. Upon addition of 8866 cells to a MadCAM-coated well, we observed a time-dependent increase in PWV shift, indicative of cell adhesion, which began to plateau at the 90-min time point. 8866 cells do not express α4β1 yet express high amounts of α4β7. We observed that the α4-specific antibody, 21/6, completely blocked the adhesion of 8866 cells to MadCAM in this assay, which would suggest that the PWV shift that was observed was not due to nonspecific or other protein–protein interactions but due predominantly to the interaction of 8866 cells with MadCAM (**Fig. 1**). In addition, a β7-specific antibody also blocked the interaction of 8866 cells to MadCAM in this assay (data not shown). A small amount of PWV shift was observed from the incubation of 8866 cells onto a well coated with only Fc antibody in the absence of MadCAM.

Determining the effect of cell density, Fc capture antibody, and MadCAM plating concentrations on assay performance

To better understand the parameters of the assay and to ensure that we are operating close to optimal assay conditions for screening compounds, we have investigated the effect of cell density, Fc capture antibody, and MadCAM plating concentrations on PWV shift. The recombinant MadCAM that we used in this study has an Fc tag that is strategically placed at its C-terminus as an N-terminal tag could affect proteolytic processing. Using this Fc tag, MadCAM could be specifically captured onto the SRU BIND plate in a manner that is optimal for binding α4β7 that is expressed on 8866 cells. In this assay, the Fc capture antibody was passively immobilized on the TiO_2 plate and then washed, followed by incubation with MadCAM overnight. In **Figure 2**, we have titrated the Fc capture antibody concentration while keeping the MadCAM concentration constant at 0.3 μg/mL. Passively immobilizing a 1:500 dilution of Fc capture antibody into the TiO_2 plate to capture MadCAM markedly enhanced the PWV shift compared to the signal observed when cells would settle on BSA or passively coated MadCAM (0.3 μg/mL) alone (**Fig. 2**). Dilutions of 1:4000 or greater of the Fc capture antibody resulted in a decreased PWV shift compared to lower dilutions. These data would suggest that the Fc capture antibody correctly orientates MadCAM,

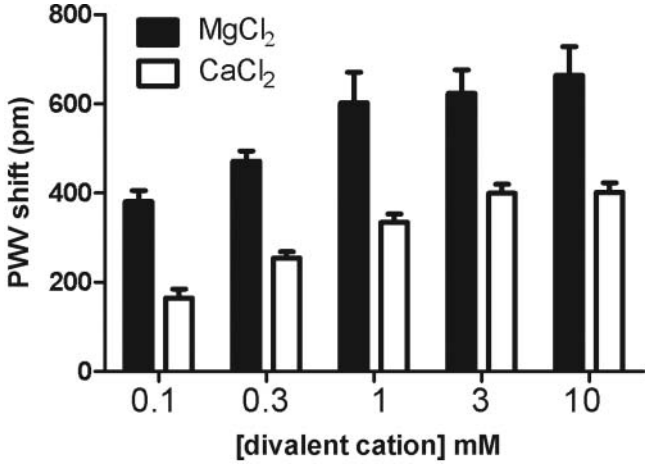

FIG. 3. Metal dependency of α4β7 interaction with MadCAM in the 8866 cell adhesion assay. 8866 cells were diluted in a buffer containing 20 mM HEPES (pH 7.4) supplemented with 140 mM NaCl. Immediately before incubation of 8866 cells in the MadCAM-coated plate, $MgCl_2$ or $CaCl_2$, at the final concentrations indicated in the figure, was added to the cell suspension. The peak wavelength value (PWV) shift after 45 min of incubation of cells in the plate was recorded and plotted. Data represent the mean ± SD, $n = 4$.

allowing optimal binding to α4β7 expressed on 8866 cells and subsequent cell adhesion.

Keeping the Fc capture antibody concentration constant at a 1:500 dilution, we next permuted the MadCAM concentrations to identify an optimal concentration range. Applying concentrations of MadCAM from 0.6 to 0.075 μg/mL in-well yielded similar signals where we began to observe a drop in PWV shift at 0.038 μg/mL concentration of MadCAM (see **Supplemental Figure S1**). For future experiments, we chose either 0.075- or 0.15-μg/mL concentrations of MadCAM, which ensured maximal signal to background.

Another parameter of relevance to investigate was the final cell density in the well where we added 10, 20, 40, 60, 80, and 120×10^3 cells to MadCAM-coated wells and plotted PWV shift at the 45-min time point. We observed a linear increase in PWV shift with increasing concentration of 8866 cells/well, which began to plateau at the 80×10^3 cells/well density (**Supplemental Figure S1B**). The 60×10^3 cells/well density was chosen for future experiments as it represents a compromise between a reasonable signal and the extra cell culture burden required for using higher cell densities.

Metal dependency of α4β7 interaction with MadCAM

Divalent cations have been shown to regulate the affinity of integrins for their ligands. More recently, crystallographic studies have revealed the absolute requirement of divalent ions for ligand binding where the affinities of these interactions were differentially regulated by Mg^{2+}, Ca^{2+}, and Mn^{2+}.[26] In **Figure 3**, we have investigated the effects of Mg^{2+} and Ca^{2+} ions in their ability to regulate adhesion of α4β7-expressing 8866 cells to a MadCAM-coated TiO_2 plate. We observed that Mg^{2+} alone was more effective in promoting adhesion than Ca^{2+} at each concentration tested (**Fig. 3**).

Dose–response curves generated using a standard small-molecule inhibitor of 8866 cell adhesion to MadCAM

To help validate our assay, we measured the kinetics of 8866 cell adhesion to MadCAM in the presence of increasing concentrations of compound 1, a standard inhibitor of α4β7-mediated cell adhesion to MadCAM (**Fig. 4A**). In this experiment, the PWV shift of 8866 cells, in the presence of increasing concentrations of compound 1, was recorded at 5-min intervals where we observed that compound 1 dose-dependently inhibited adhesion of 8866 cells to MadCAM. Choosing the 45-min time point for endpoint analysis, which is in the linear region of the PWV shift in this assay, we generated a dose–response curve characterized by an IC_{50} for inhibition of 8866 cell adhesion of 238 nM (**Fig. 4B**). This value compared closely to the IC_{50} of 430 nM that was generated using the manual cell adhesion assay format (data not shown).

Correlation and variability between manual and SRU BIND assay formats

Currently, most assays to monitor cell adhesion are performed in a manual workstation mode, whereas the SRU BIND assay is performed in a label-free homogeneous format that records PWV shift as a readout parameter. One component in validating data generated using a novel technology platform is to compare them to data generated using an established standard format. In **Figure 5A**, we have taken a battery of compounds exhibiting low, medium, and high potency in the manual cell adhesion assay format and compared these IC_{50} values to those obtained with the SRU BIND assay format. A correlation plot between IC_{50} values calculated using the two formats yielded a correlation coefficient of 0.86. We also quantified variability in terms of Z' between manual and SRU BIND formats where the Z' value for the SRU BIND format was calculated to be 0.61, and the Z' for the manual format was 0.56. Assay consistency with the SRU BIND format was investigated by testing the same battery of compounds on two different test occasions where we observed a correlation coefficient of 0.87, as shown in **Figure 5B**. The one circled point in **Figure 5B** was the result of a compound that we later found to be unstable when kept at –20 °C.

Applicability of the SRU BIND platform to measuring α4β1 adhesion to the vascular cell adhesion molecule

Although the SRU BIND platform has demonstrated excellent utility in measuring the adhesion of 8866 cells expressing α4β7 to MadCAM, we wanted to determine whether this technique could

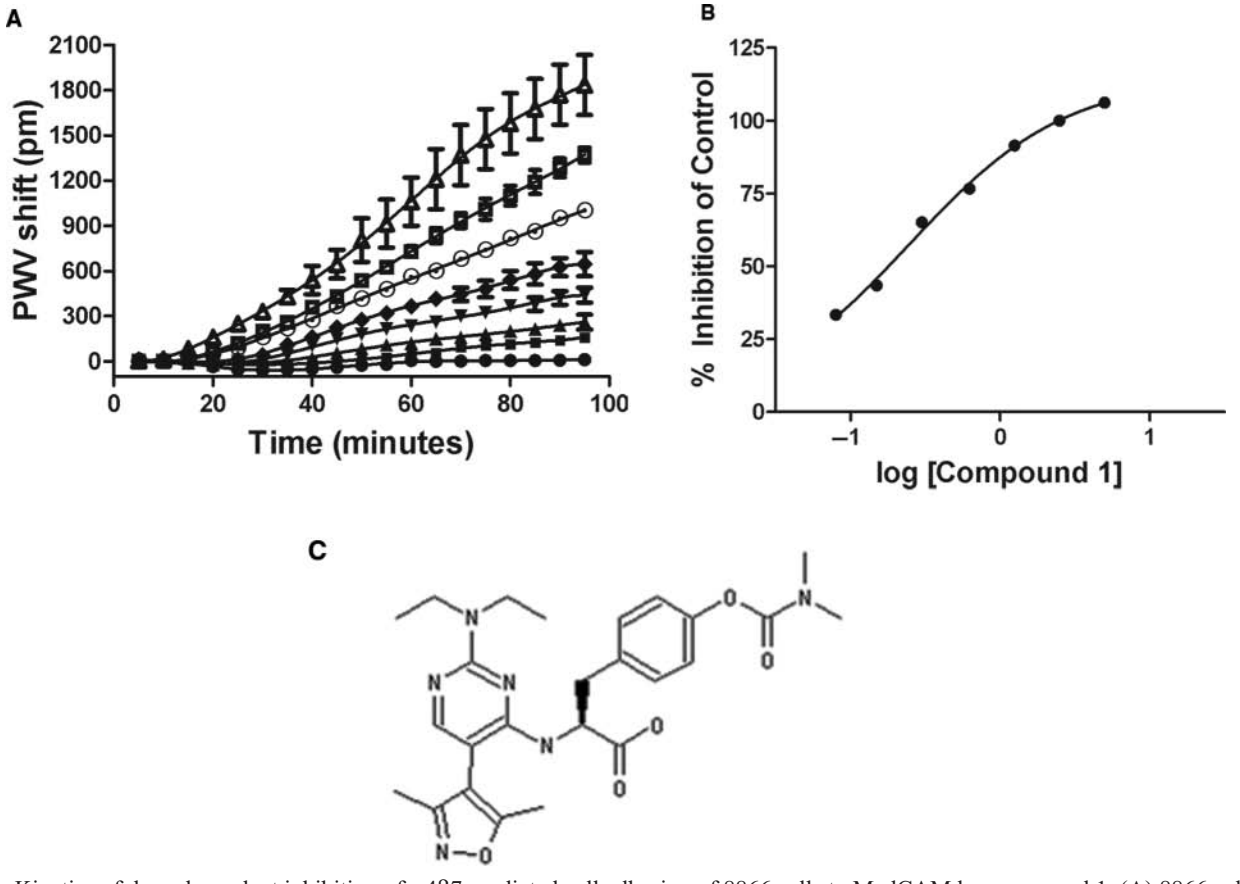

FIG. 4. Kinetics of dose-dependent inhibition of α4β7-mediated cell adhesion of 8866 cells to MadCAM by compound 1. (**A**) 8866 cells were incubated alone (△) or with 0.08 μM compound (□), 0.15 μM (○), 0.3 μM (◆), 0.625 μM (▼), 1.25 μM (▲), 2.5 μM (■), and 5 μM (●), before addition to a MadCAM-coated plate. Peak wavelength value (PWV) shifts were recorded for 90 min using the SRU BIND reader. All data were normalized to 8866 cell adhesion to a bovine serum albumin–blocked plate alone. Data represent the mean ± SD, $n = 4$. This experiment has been repeated on more then 10 different occasions with similar results. (**B**) The PWV shift at the 45-min time point from the incubation of 8866 cells with each compound concentration shown in (**A**) recorded. These data were used to plot a dose–response curve showing inhibition of 8866 cell adhesion to the MadCAM-coated plate. Data were plotted as % inhibition of control PWV shift where control was the amount of PWV shift observed when 8866 cells alone (without compound) adhered to the MadCAM-coated biosensor. (**C**) Structure of compound 1.

also measure cell adhesion of other integrins to their binding partners. Thus, we have immobilized vascular cell adhesion molecule (VCAM)–Fc onto a TiO_2 BIND plate similar to how we have captured MadCAM onto the TiO_2-coated biosensor. Jurkat cells endogenously express α4β1, which has been shown to interact strongly with VCAM, which is thought to mediate T cell infiltration into the central nervous system (CNS).[21,25] Upon addition of Jurkat cells into the VCAM-coated well, we observed a time-dependent enhancement of PWV shift indicative of cell adhesion, which began to plateau after 60 minutes (**Fig. 6**). In contrast, we observed only a small increase in PWV shift when 8866 cells were added to wells coated with BSA or Fc capture antibody alone (**Fig. 6**). The interaction of Jurkat cells with VCAM was completely blocked with an α4 blocking antibody at 15 μg/mL concentration (data not shown).

Imaging of cell adhesion and attachment with the SRU BIND Scanner

The SRU BIND Scanner allows for imaging of cells at the biosensor surface. Imaged cells are shown as light blue spots in **Figure 7A**. In row 1, compound 1 dose-dependently decreased the number of light blue spots imaged. Similarly, an α4 blocking antibody also dose-dependently decreased the number of cells imaged by the scanner (data not shown). Row 2 illustrates background levels of imaged cells in the absence of MadCAM. We would expect that in the absence of MadCAM, we should observe a similar amount of cells to be imaged at different compound concentrations, which is what we observed (**Fig. 7A**, row 2). For all objects that were determined to be cells and imaged by the scanner in a well, cell adhesion strength, which

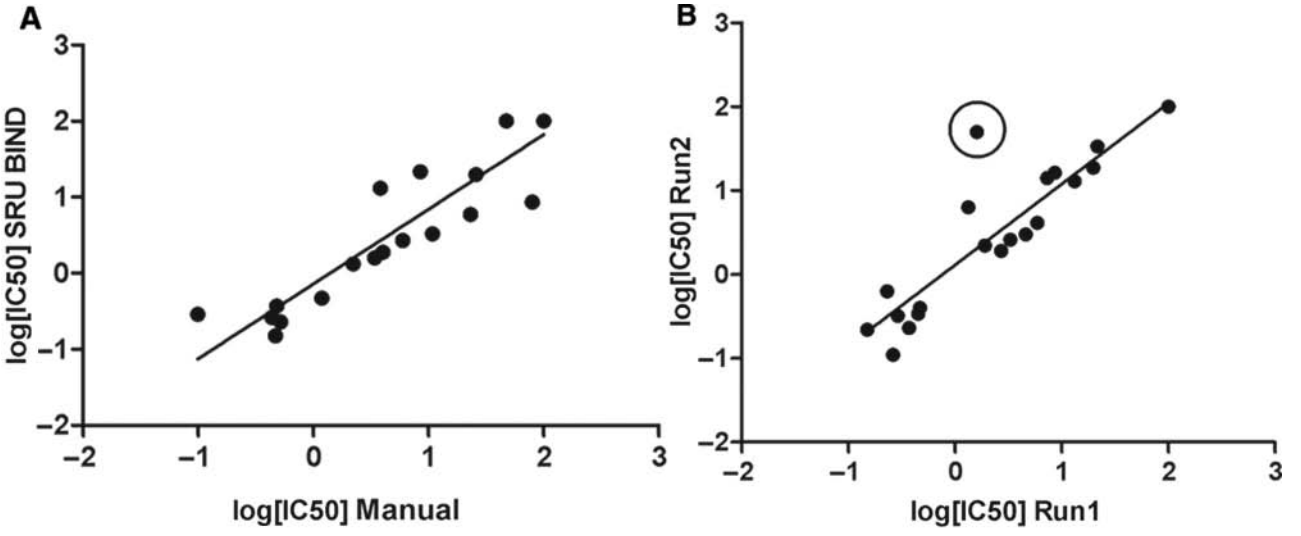

FIG. 5. (**A**) Correlation between the manual cell adhesion assay and SRU BIND assay formats. Using a battery of test compounds that included compounds of low, medium, and high potency, IC_{50} values were determined by both manual and SRU BIND assay formats as described in Materials and Methods and were plotted against each other, resulting in a graph yielding a correlation coefficient of 0.86. (**B**) Low assay variation observed with the SRU BIND platform. Using a battery of compounds of low, medium, or high potency, IC_{50} values were determined, as described in Materials and Methods, on two separate test occasions using the SRU BIND format and plotted against each other, yielding a correlation coefficient of 0.87.

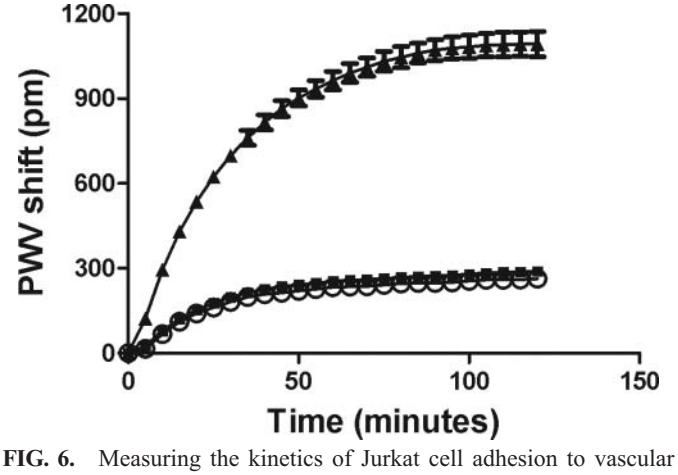

FIG. 6. Measuring the kinetics of Jurkat cell adhesion to vascular cell adhesion molecule (VCAM) using the SRU BIND platform. Jurkat cells endogenously expressing α4β1 were added to each well of a SRU BIND plate under the following conditions: (■) bovine serum albumin blocked plate only, (○) Fc capture antibody only, and (▲) Fc capture antibody + 0.1 μg/mL VCAM. Data represent the mean ± SD, $n = 4$.

is defined by the intensity of the object imaged, was determined for each cell and averaged in a well. A dose–response curve of cell adhesion strength was calculated from each concentration of compound 1 used in **Figure 7A** and plotted in **Figure 7B**. Compound 1 dose-dependently decreased cell adhesion strength with an IC_{50} of 340 nM. The question remains whether cells that are imaged by the scanner represent cells that have passively settled onto the surface or mostly cells that have adhered to MadCAM. Using data obtained from brightfield analysis, we determined by manual counting that the number of cells that have settled onto the surface of the biosensor is the same whether or not compound 1 or α4 blocking antibody is present (**Supplemental Figure S2** and data not shown), suggesting that the scanner predominantly images cells that have adhered to MadCAM.

DISCUSSION

There can be an advantage to developing screening assays that recapitulate as close as possible the relevant in vivo biology of the system that you are attempting to model. T cells expressing α4β7 are directed into the gut as a result of the interaction of α4β7 with the gut lining, which expresses MadCAM. In this article, we have described a label-free, homogeneous, functional cellular assay measuring α4β7-mediated cell adhesion of 8866 cells to MadCAM in a format that is amenable to HTS. This cell-based functional screening assay could represent an advantage over non-cell-based biochemical assays in identifying compounds that block the interaction of a recombinant expressed α4β7 integrin with MadCAM. This system has shown the potential for wide applicability in measuring integrin-based cell adhesion events where, in addition to measuring 8866 cell adhesion to MadCAM, we have also characterized the kinetics of Jurkat cell adhesion to VCAM

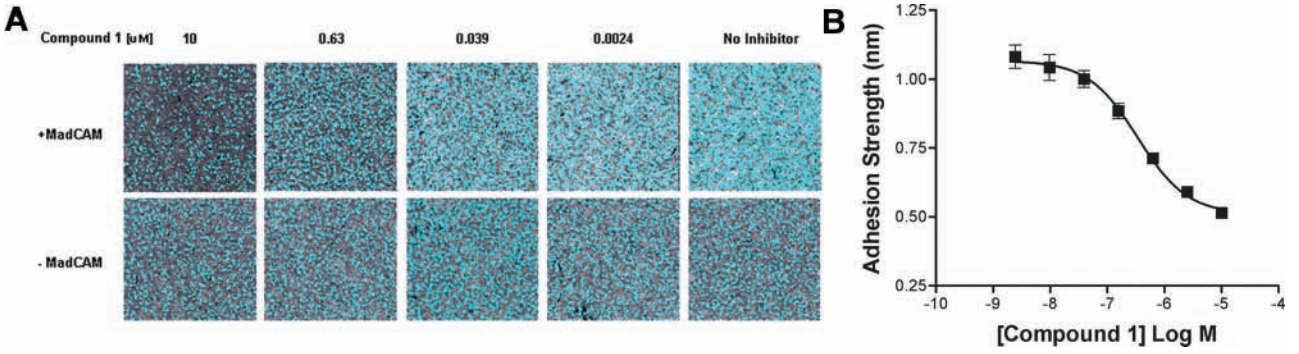

FIG. 7. (**A**) Label-free imaging allows for visualization of cell adhesion and its inhibition by small-molecule antagonist. 8866 cells (60K cells/well) were added to a MadCAM-coated TiO_2 plate in the presence or absence of varying concentrations of compound 1 as indicated in the figure. After a 45-min incubation, images were recorded using the SRU BIND scanner. Cell images (light blue spots) were generated by thresholding the high-resolution, label-free signals measured on the BIND Scanner as described in Materials and Methods. In row 2, background 8866 cell binding to a plate coated solely with bovine serum albumin is shown. (**B**) Small-molecule antagonist compound 1 reduces the strength of cell adhesion of 8866 cells to MadCAM. 8866 cells incubated in the absence or presence of varying concentrations of compound 1 (as in **A**) were added to a MadCAM-coated BIND plate, and at the 45-min time point, the strength of cell adhesion was determined as described in Materials and Methods and plotted at the concentrations indicated to generate a dose–response curve.

(**Fig. 6**). Aberrant cell adhesion caused by activation of integrins can play a role in mediating a number of pathologies, including coronary heart disease, cancer, and inflammatory diseases.[25] Thus, the applicability of this technique toward measuring adhesion in different cellular systems with different integrins and their binding partners could pave the way for the identification of new classes of integrin antagonists in the future.

The high degree of correlation between the SRU BIND format and the manual assay format in running a battery of standard and negative control compounds suggests that this novel platform offers a reliable readout for measuring cell adhesion and inhibition by small molecules (**Fig. 5A,B**). Similar to what has been shown by other investigators using other manual assay formats,[26,27] divalent ions were shown to dramatically affect cell adhesion in this assay as well (**Fig. 3**). Although the calculated Z′ values for both assays were comparable, we did observe less variability in IC_{50} determinations using the SRU BIND format for some historically problematic compounds that yielded inconsistent IC_{50} determinations using the manual assay format (data not shown).

The readout parameter for the label-free SRU BIND format is PWV shift. How does a shift in PWV reflect cell adhesion? Some insight into answering that question is provided by the data in **Figure 7A**, generated using the SRU BIND Scanner, which shows images of 8866 cells at the biosensor surface. The BIND Scanner essentially takes a point-by-point PWV determination of cells in the well and converts that data to a line image. Compound 1 and an α4 blocking antibody dose-dependently decreased the number of imaged cells (**Fig. 7A** and data not shown). In contrast, images created using brightfield analysis show that an approximately equal number of cells have settled onto the biosensor surface, whether blocking antibody or compound was present or not (**Supplemental Figure S2**). The images in **Figure 7A** and **Supplementary Figure S2** would suggest that the large PWV shift measured by the biosensor on the SRU BIND Reader after addition of 8866 cells to MadCAM-coated wells (**Fig. 1**) is predominantly due to cellular adhesion events mediated by α4β7 interaction with MadCAM and not passive settling onto the biosensor, which does not elicit as large a magnitude of response or signal in this assay format.

Integrin signaling is closely coordinated and linked to growth factor signaling, where both pathways can modulate common signal transduction components. Activation of the canonical Ras-Raf-Mek-ERK pathway by growth factors is modulated or enhanced by integrins.[28,29] Similarly, GPCRs, receptor tyrosine kinases (RTKs), and ion channels have been shown to modulate integrin affinity in what is known as inside-out signaling.[5,6] Both the SRU BIND and impedance-based label-free systems have been shown to be successful in measuring responses to GPCRs in agonist or antagonist modes.[30] By analogy to what we have observed in this study, PWV shifts that occur as a result of GPCR or ion channel modulation most likely result, in part, from GPCR-induced alterations of cellular adhesion at the biosensor surface. Thus, this platform could be useful for measuring activation or inhibition of any signaling pathway that can modulate the integrin system.

Thus, here we have developed a robust, label-free, and homogeneous assay to measure cellular adhesion of α4β7-expressing 8866 cells to MadCAM using the SRU BIND technology. This assay was validated using an α4 blocking antibody and standard compounds. This technology is widely

applicable to measuring cellular adhesion mediated by other integrins to their binding partners and is amenable to HTS and thus represents an alternative assay platform for cell adhesion assays that will allow for the identification of new compounds that will be of therapeutic benefit in inflammatory diseases and cancer.

ACKNOWLEDGMENT

We acknowledge Linnea Diep and David Nakamura for their expert technical assistance and also Michael Bradshaw for critical evaluation of the manuscript. We also acknowledge Rafael Fernandez and Mann Shoffner for thoughtful discussions.

REFERENCES

1. Schwartz, M. A.; Schaller, M. D.; Ginsberg, M. H. Integrins: Emerging Paradigms of Signal Transduction. *Annu. Rev. Cell Dev. Biol.* **1995**, *11*, 549–599.
2. Hynes, R. Integrins: Bidirectional, Allosteric Signaling Machines. *Cell* **2002**, *110*, 673–687.
3. Calderwood, D. A. Integrin Activation. *J. Cell Sci.* **2004**, *117*, 657–666.
4. Shimaoka, M.; Springer, T. A. Therapeutic Antagonists and Conformational Regulations of Integrin Function. *Nat. Rev. Drug Discov.* **2003**, *2*, 703–716.
5. Faull, R. J.; Ginsberg, M. H. Inside-Out Signaling through Integrins. *J. Am. Soc. Nephrol.* **1996**, *7*, 1091–1097.
6. Hughes, P. E.; Pfaff, M. Integrin Affinity Modulation. *Trends Cell Biol.* **1998**, *8*, 359–364.
7. Shattil, S. J.; Kashiwagi, H.; Pampori, N. Integrin Signaling: The Platelet Paradigm. *Blood* **1998**, *91*, 2645–2657.
8. Steinhubl, S. R.; Moliterno, D. J. The Role of the Platelet in the Pathogenesis of Atherothrombosis. *Am. J. Cardiovasc. Drugs* **2005**, *5*, 399–408.
9. Cram, E. J.; Schwarzbauer, J. E. The Talin Wags the Dog: New Insights into Integrin Activation. *Trends Cell Biol.* **2004**, *14*, 55–57.
10. Shamri, R.; Grabovsky, V.; Gauguet, J. M.; Feigelson, S.; Manevich, E.; Kolanus, W.; Robinson, M. K.; Staunton, D. E.; von Andrian, U. H.; Alon, R. Lymphocyte Arrest Requires Instantaneous Induction of an Extended LFA-1 Conformation Mediated by Endothelium-Bound Chemokines. *Nat. Immunol.* **2005**, *6*, 497–506.
11. Kinashi, T. Intracellular Signaling Controlling Integrin Activation in Lymphocytes. *Nat. Rev. Immunol.* **2005**, *5*, 546–559.
12. Ginsberg, M. H.; Partridge, A.; Shattil, S. J.; Integrin Regulation. *Curr. Opin. Cell Biol.* **2005**, *17*, 509–516.
13. Shattil, S. J.; Newman, P. J.; Integrins: Dynamic Scaffolds for Signaling and Adhesion in Platelets. *Blood* **2004**, *104*, 1606–1615.
14. Assoian, R. K.; Schwartz, M. A. Coordinate Signaling by Integrins and Receptor Tyrosine Kinases in the Regulation of G1 Phase Cell-Cycle Progression. *Curr. Opin. Genet. Dev.* **2001**, *11*, 48–53.
15. Giancotti, F. G.; Ruoslahti, F. Integrin Signaling. *Science* **1999**, *285*, 1028–1032.
16. Vijayan, K. V.; Goldschmidt-Clermont, P. J.; Roos, C.; Bray, P. F. The P1A2 Polymorphism of Integrin β3 Enhances Outside-in Signaling and Adhesive Functions. *J. Clin. Invest.* **2000**, *105*, 793–802.
17. Bauer, M.; Brakebusch, C.; Coisne, C.; Sixt, M.; Wekerle, H.; Engelhardt, B. b1 Integrins Differentially Control Extravasation of Inflammatory Cell Subsets into the CNS during Autoimmunity. *Proc. Natl. Acad. Sci. U. S. A.* **2009**, *106*, 1920–1925.
18. Braun, C.; Zahn, R.; Martin, K.; Albert, E.; Folwaczny, C. Polymorphisms of the ICAM-1 Gene Are Associated with Inflammatory Bowel Disease, Regardless of the p-ANCA Status. *Clin. Immunol.* **2001**, *101*, 357–360.
19. Reinmuth, N.; Liu, W.; Ahmad, S. A.; Fan, F.; Stoeltzing, O.; Parikh, A. A.; Bucana, C. D.; Gallick, G. E.; Nickols, M. A.; Westlin, W. F.; ET AL. αvβ3 Integrin Antagonist S247 Decreases Colon Cancer Metastasis and Angiogenesis and Improves Survival in Mice. *Cancer Res.* **2003**, *63*, 2079–2087.
20. Von Andrian, U. H.; Engelhardt, B. α4 Integrins as Therapeutic Targets in Autoimmune Disease. *N. Engl. J. Med.* **2003**, *348*, 68–72.
21. Davenport, R. J.; Munday, J. R. Alpha4-Integrin Antagonism: An Effective Approach for the Treatment of Inflammatory Diseases? *Drug Discov. Today* **2007**, *12*, 569–576.
22. Polman, C. H.; O'Connor, P. W.; Havrdova, E.; Hutchinson, M.; Kappos, L.; Miller, D. H.; Phillips, J. T.; Lublin, F. D.; Giovannoni, G.; Wajgt, A.; et al. A Randomized, Placebo-Controlled Trial of Natalizumab for Relapsing Multiple Sclerosis. *N. Engl. J. Med.* **2006**, *354*, 899–910.
23. Vanderslice, P.; Woodside, D. G. Integrin Antagonists as Therapeutics for Inflammatory Diseases. *Expert Opin. Investig. Drugs* **2006**, *15*, 1235–1255.
24. Cunningham, B.; Li, P.; Lin, B.; Pepper, J. Colorimetric Resonant Reflection as a Direct Biochemical Assay Technique. *Sensors Actuators* **2001**, *4120*, 1–13.
25. Newham, P.; Craig, S. E.; Seddon, G. N.; Schofield, N. R.; Rees, A.; Edwards, R. M.; Jones, E. Y.; Humphries, M. J. α4 Integrin Binding Interfaces on VCAM-1 and MadCAM-1. *J. Biol. Chem.* **1997**, *272*, 19429–19440.
26. Chen, J. F.; Salas, A.; Springer, T. A. Bistable Regulation of Integrin Adhesiveness by a Bipolar Metal Ion Cluster. *Nat. Struct. Biol.* **2003**, *10*, 995–1001.
27. Tidswell, M.; Pachynski, R.; Wu, S. W.; Qiu, S.-Q.; Dunham, E.; Cochran, N.; Briskin, M. J.; Kilshaw, P. J.; Lazarovits, A. I.; Andrew, D. P., et al. Structure Function Analysis of the Integrin b7 Subunit: Identifications of Domain Involved in Adhesion to MadCAM-1. *J. Immunol.* **1997**, *159*, 1497–1505.
28. Del Pozo, M. A.; Price, L. S.; Alderson, N. B.; Ren, X. D.; Schwartz, M. A. Adhesion to the Extracellular Matrix Regulates the Coupling of the Small GTPase RAC to Its Effector PAK. *EMBO J.* **2000**, *19*, 2008–2014.
29. Walsh, C. T.; Stupack, D.; Brown, J. H. G Protein-Coupled Receptors Go Extracellular: RhoA Integrates the Integrins. *Mol. Interv.* **2008**, *8*, 165–173.
30. Peters, M. F.; Vaillancourt, F.; Heroux, M.; Valiquette M.; Scott, C. W. Comparing Label-Free Biosensors for Pharmacological Screening with Cell-Based Functional Assays. *Assay Drug Dev. Technol.* **2010**, *8*, 219–227.

Address correspondence to:
Michael P. Bova, Ph.D.
Department of Biology
Elan Pharmaceuticals
1000 Gateway, South San Francisco, CA 94080

E-mail: michael.bova@elan.com